Supplemental Figures

Supplement Figure 1: Number of differentially expressed probe sets.
The number of differentially expressed probe sets exhibiting a log_2-fold change of >1 (>2-fold change) and an adjusted p-value of <0.05 between infected and mock-infected mice for WT (WT), single *Irf3*$^{-/-}$ (Irf3) and *Irf7*$^{-/-}$ (Irf7) KO, and *Irf3*$^{-/-}$*Irf7*$^{-/-}$DKO (Irf3/7) mice at day 3 pi with $2x10^3$ FFU PR8M were determined by LIMMA. Up-regulated probe sets are shown in red, down-regulated in blue. n = 3 for all groups.

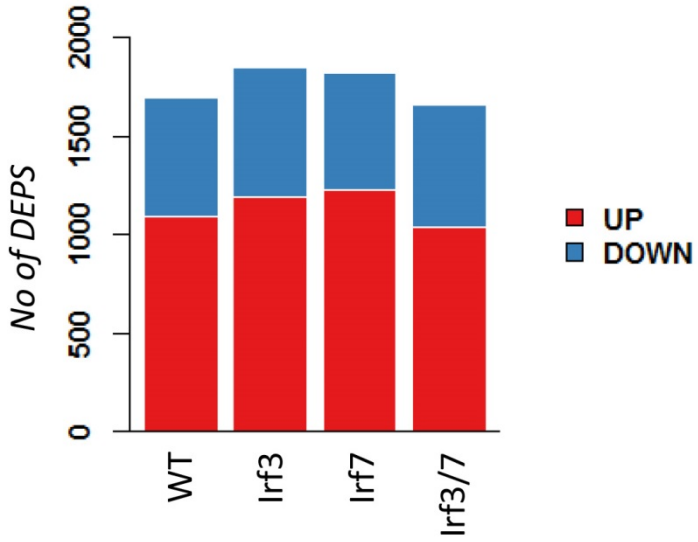

Supplement Figure 2: Quantitative analysis of epithelial cell damage and cellular infiltrates in histological sections.

Five WT C57BL/6J and four Irf3$^{-/-}$Irf7$^{-/-}$ DKO female mice at the age of 8-12 weeks were infected intranasally with 2x10^5 FFU PR8M (H1N1) influenza A virus. The percentage of bronchiolar structures affected by epithelial cell necrosis (a) and the ratio of monocytic to granulocytic infiltration (b) were determined on sections stained with haematoxylin/eosin. The number of virus infected bronchiolar epithelial cells was counted on sections immunohistochemically stained with an anti-influenza nucleoprotein antibody (c). Data represents mean values +/- SEM. Irf3$^{-/-}$Irf7$^{-/-}$ mice showed significantly higher epithelial damage and infiltration of granulocytic cells compared to WT mice as well as significantly more virus infected cells (*p<0.05). Significances were calculated using Mann-Whitney U tests. Irf3/7$^{-/-}$: Irf3$^{-/-}$Irf7$^{-/-}$ mutant genotypes.

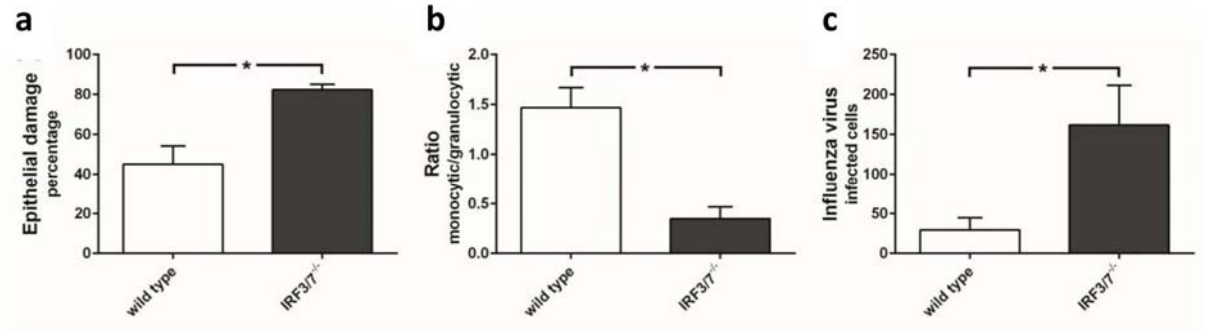

Supplement Figure 3: Gene expression changes for individual genes.
Changes in the expression levels of probe sets representing interferon genes (*Ifn's*) (a,b) and interferon-stimulated genes (*Isg's, Ifit's, Ifitm's Mx's, Oas's*) (c-f) in lungs of WT, single KO and DKO mice infected with $2x10^3$ FFU PR8M at day 3 pi Expression values represent normalized log_2 transformed signal intensities relative to expression levels in mock-infected control mice at day 3 post treatment. n = 3 for all groups. md3: mock infected mice at day3 post treatment, d3 and d5: infected mice at day 3 and 5 p.i., respectively. wt, wild type; Irf3, $Irf3^{-/-}$; Irf7: $Irf7^{-/-}$ and Irf37: $Irf3^{-/-}Irf7^{-/-}$ genotypes, respectively.

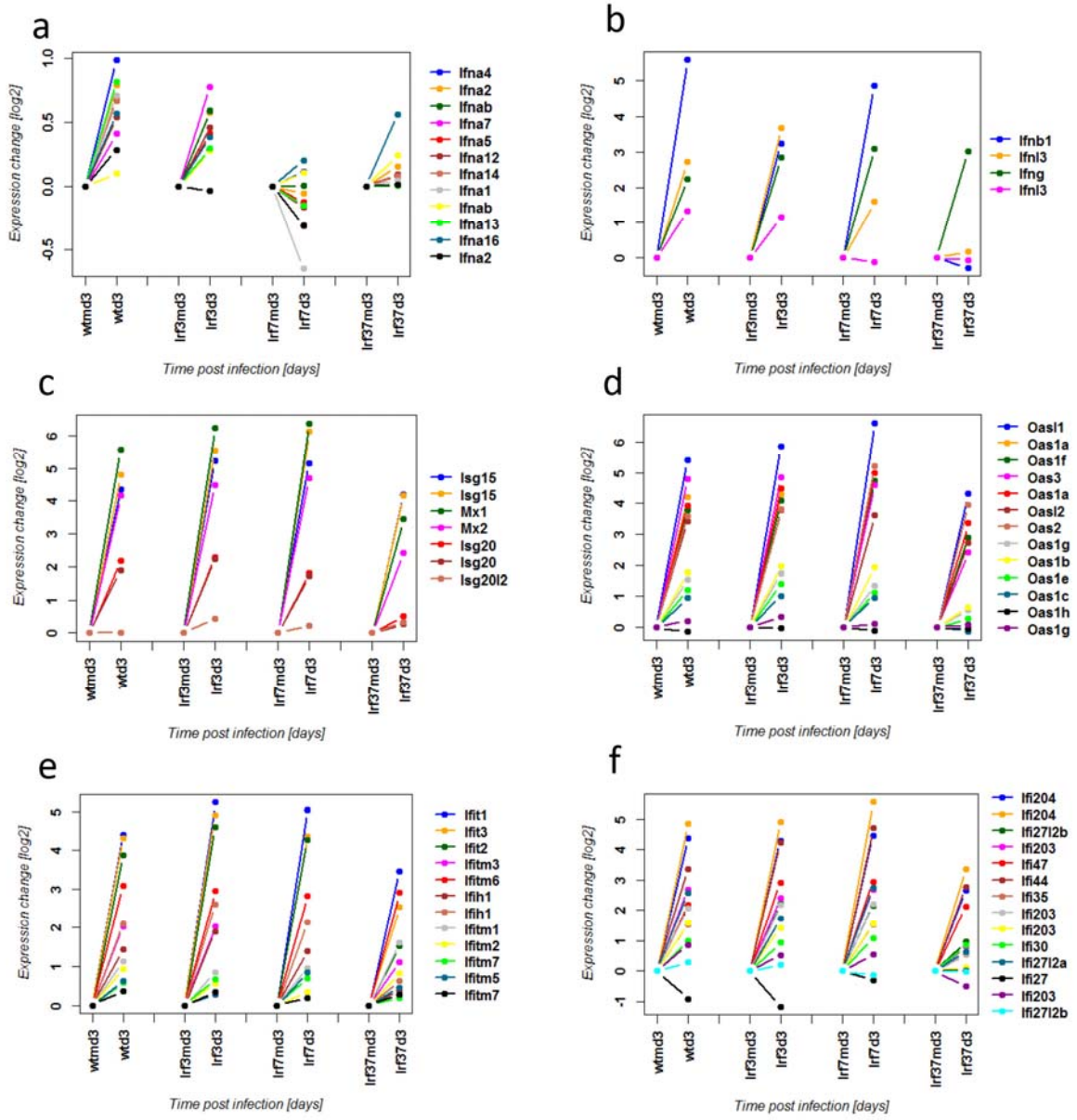

Supplement Figure 4: Validation of gene expression changes by quantitative RT-PCR.

The y-axis shows the fold-change as $\log_2$ using the $\Delta\Delta$CT method from qRT-PCR analyses of selected genes from the host chemokine-cytokine, interferon-stimulated genes (ISGs), JNK pathway and adaptive immune response. All genes tested showed the same trends of up- or down-regulation in DKO mutants, except for *Atf2* where a difference was seen for the delta-DKO-minus-WT values (0.223 in arrays and -0.066 in qRT-PCR). md3: mock infected mice at day3 post treatment, d3 and d5: infected mice at day 3 and 5 p.i., respectively. WT, wild type; Irf3: $Irf3^{-/-}$; Irf7: $Irf7^{-/-}$ and Irf3x7: $Irf3^{-/-}Irf7^{-/-}$ genotypes, respectively

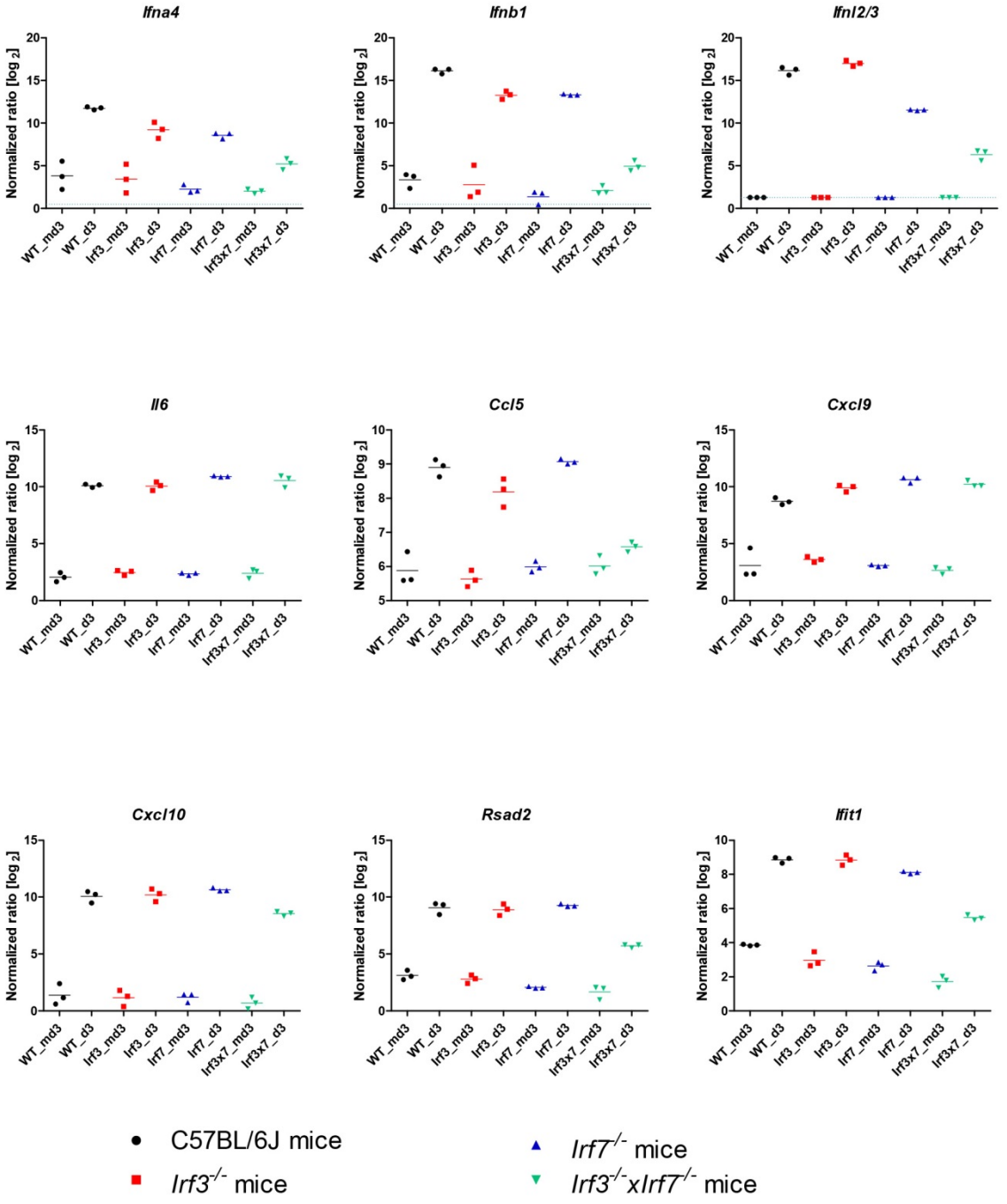
Ifna4
Ifnb1
Ifnl2/3
Il6
Ccl5
Cxcl9
Cxcl10
Rsad2
Ifit1
Normalized ratio [log 2]
WT_md3
WT_d3
Irf3_md3
Irf3_d3
Irf7_md3
Irf7_d3
Irf3x7_md3
Irf3x7_d3
C57BL/6J mice
Irf3-/- mice
Irf7-/- mice
Irf3-/-xIrf7-/- mice

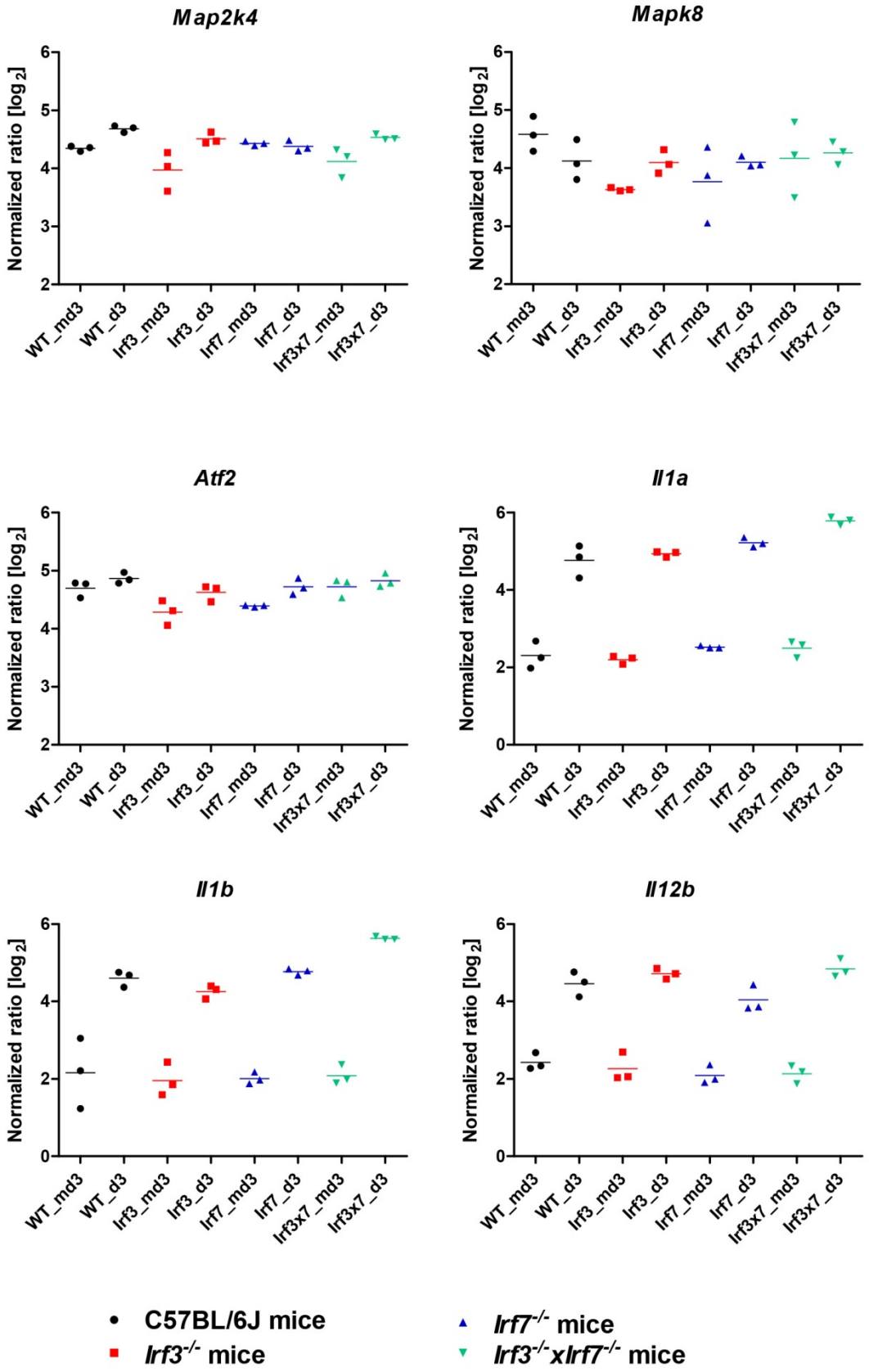
Map2k4
Mapk8
Atf2
Il1a
Il1b
Il12b
Normalized ratio [log 2]
WT_md3
WT_d3
Irf3_md3
Irf3_d3
Irf7_md3
Irf7_d3
Irf3x7_md3
Irf3x7_d3
C57BL/6J mice
Irf7-/- mice
Irf3-/- mice
Irf3-/-xIrf7-/- mice

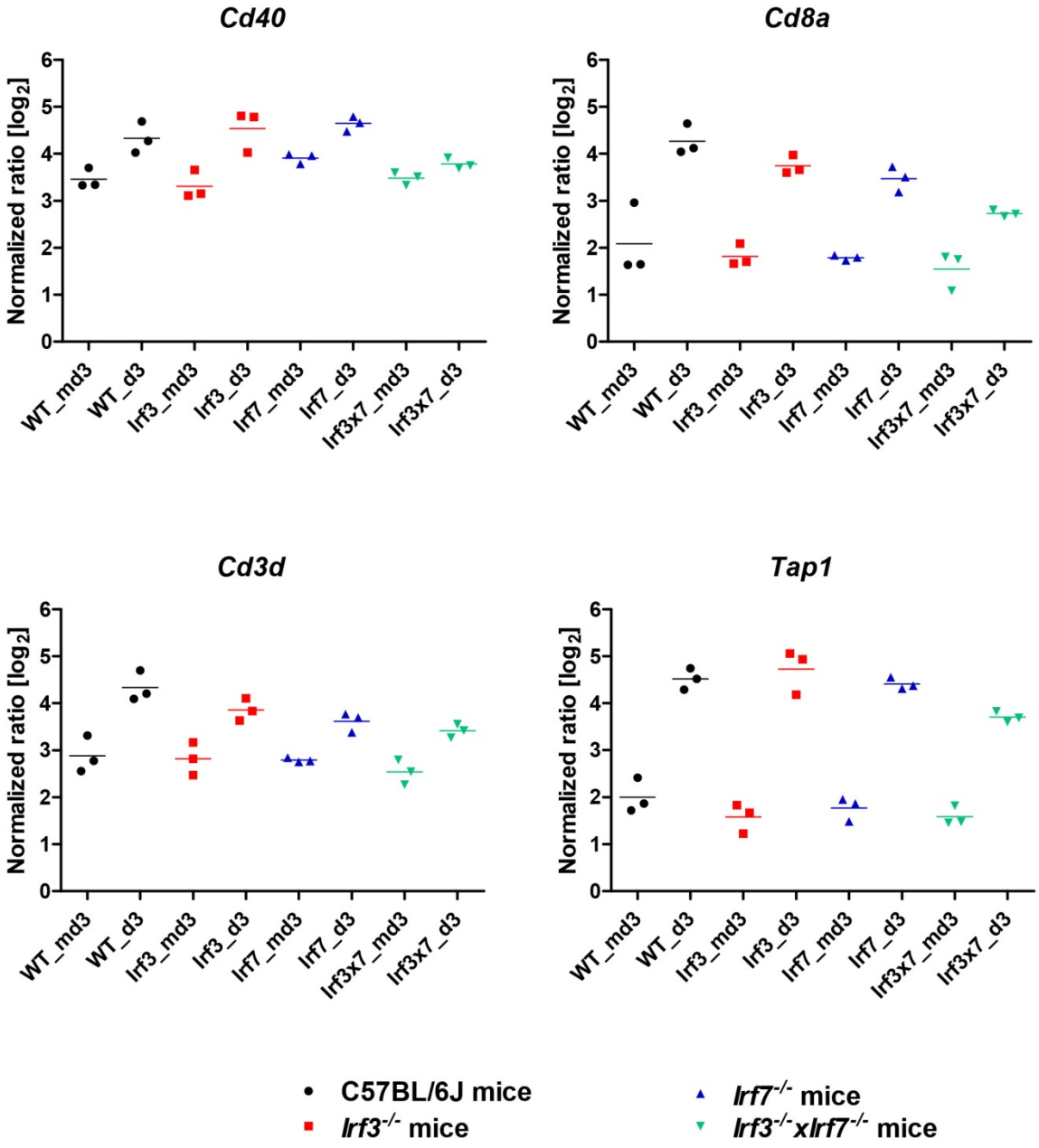
Cd40
Cd8a
Cd3d
Tap1
Normalized ratio [log2]
0
1
2
3
4
5
6
WT_md3
WT_d3
Irf3_md3
Irf3_d3
Irf7_md3
Irf7_d3
Irf3x7_md3
Irf3x7_d3
C57BL/6J mice
Irf7-/- mice
Irf3-/- mice
Irf3-/-xIrf7-/- mice

Supplement Table 1: Primer sequences for qRT-PCR

No.	Primer name	Sequence (5' - 3')	Note
1	Ifna4-F	CAAGCCATCCTTGTGCTAAGAG	*
2	Ifna4-R	GGAGGTTCCTGCATCACACAG	*
3	Ifnb1-F	CCAGCTCCAAGAAAGGACGAAC	(Takaki et al., 2013, modified)
4	Ifnb1-R	CTTCTCCGTCATCTCCATAGGG	(Daffis et al., 2007)
5	Ifnl2/3-F	GCCACATTGCTCAGTTCAAG	*
6	Ifnl2/3-R	GCACCTCATGTCCTTCTCAAG	*
7	Il6-F	TACTTCACAAGTCCGGAGAGG	*
8	Il6-R	TCCACGATTTCCCAGAGAAC	*
9	Ccl5-F	TCGTGTTTGTCACTCGAAGG	*
10	Ccl5-R	CCCTCTATCCTAGCTCATCTCC	(Lazear et al., 2013, modified)
11	Cxcl9-F	CTCGGCAAATGTGAAGAAGC	*
12	Cxcl9-R	GACGACTTTGGGGTGTTTTG	*
13	Cxcl10-F	GGTCTGAGTGGGACTCAAGG	*
14	Cxcl10-R	GTGGCAATGATCTCAACACG	*
15	Rsad2-F	ACACAGCCAAGACATCCTTCG	(Lazear, 2013, modified)
16	Rsad2-R	CAAGTATTCACCCCTGTCCTG	(Lazear, 2013)
17	Ifit1-F	GAGCCAGAAAACCCTGAGTAC	(Daffis et al., 2007, modified)
18	Ifit1-R	TTAACCGGACAGCCTTCCTC	*
19	Map2k4_F	CAGTGGACAGCTTGTGGACT	*
20	Map2k4_R	CTCCAGACATCAGAGCGGAC	*
21	Mapk8_F	GAGAAACTGTTCCCCGATGTGC	*
22	Mapk8_R	TCCCTCTCATCTAACTGCTTGTC	*
23	Atf2_F	GCCATGGCAGTGGATTGGTTAG	*
24	Atf2_R	GACGGCCACTTGTATTTTGGG	*
25	Ila_F	CTGCCATTGACCATCTCTCTCTG	*
26	Ila_R	GACGTTGCTGATACTGTCACC	*
27	Il1b-F	GGGCCTCAAAGGAAAGAATC	*
28	Il1b-R	TACCAGTTGGGGAACTCTGC	*
29	Il12b_F	CTTTGTTCGAATCCAGCGCAAG	*
30	Il12b_R	GTAATAGCGATCCTGAGCTTGC	*
31	Cd40_F	GCTATGGGGCTGCTTGTTGA	(Morgado et al., 2014)
32	Cd40_R	ATGGGTGGCATTGGGTCTTC	*
33	Cd8a_F	TCGTGCCAGTCCTTCAGAAAG	*
34	Cd8a_R	TATCACAGGCGAAGTCCAATCC	*
35	Cd3d_F	ACACTCAACTTGGGCAAAGG	*
36	Cd3d_R	CACACAGTTCTGGCACATTCG	*
37	Tap_F	GTTCTCTACCAGCTTCAGTTCACC	*
38	Tap_R	GGAACTCCACAAGGCCTTTCATG	*
39	Rpl4-F	CGAAAAGGGAGAGTCATCTGG	*
40	Rpl4-R	CCAATTCACTGACGGCATAGG	*

Note: * These primers were designed based on ENSEMBL mouse database, Primer3Plus and Primer-BLAST (http://www.ensembl.org/Mus_musculus/Info/Index, http://www.primer3plus.com, and http://www.ncbi.nlm.nih.gov/tools/primer-blast).

References

Daffis, S. et al. (2007). Cell-specific IRF-3 responses protect against West Nile virus infection by interferon-dependent and -independent mechanisms. *PLoS Pathog, 3*(7), e106. doi: 10.1371/journal.ppat.00301

Lazear, H. et al. (2013). IRF-3, IRF-5, and IRF-7 coordinately regulate the type I IFN response in myeloid dendritic cells downstream of MAVS signaling. *PLoS Pathog, 9*(1), e1003118. doi: 10.1371/journal.ppat.1003118

Morgado, P. et al. (2014). Type II *Toxoplasma gondii* Induction of CD40 on infected macrophages enhances interleukin-12 responses. *Infect Immun*, 82(10), 4047–4055. doi: 10.1128/IAI.01615-14

Takaki et al. (2013). The MyD88 pathway in plasmacytoid and CD4+ dendritic cells primarily triggers type I IFN production against measles virus in a mouse infection model. *J Immunol, 191*(9), 4740-4747. doi: 10.4049/jimmunol.1301744